Impacts of SiO_2-Buried Structure on Performances of GaN-Based Vertical-Cavity Surface-Emitting Lasers

Rongbin Xu, Hidefumi Akiyama, and Baoping Zhang

***Abstract*— Numerical analysis of the optical and electrical properties of GaN-based vertical-cavity surface-emitting lasers (VCSELs) with SiO_2-buried structure were performed. The simulation results show that, as the SiO_2 layer gets thicker, threshold simply gets lower, but slope efficiency gets initially smaller and then gets larger. The mechanism of these tendencies are explained as, when the SiO_2 layer becomes thicker, a better lateral optical confinement can be achieved, while the current confinement becomes worse due to the existence of polarization electric field. Furthermore, since the injection current density is higher for VCSEL with small aperture size, the worse current confinement will result in lower slope efficiency. A proper design of SiO_2-buried structure to avoid the effect of leakage current is essentially important to achieve high-efficiency GaN-based VCSELs.**

***Index Terms*— GaN-based laser, numerical simulation vertical-cavity surface-emitting laser (VCSEL), optical and current confinement.**

I. Introduction

IN CONTRAST to edge-emitting laser diodes, some advantages of vertical-cavity surface-emitting lasers (VCSELs) were highlighted such as small mode volume, low divergent output beam, and easy array formation. These unique properties have made VCSELs ubiquitous in our daily lives, such as optical data storage, lighting, and laser printers [1], [2]. At present, GaAs-based long-wavelength infrared (IR) VCSELs have been commercialized due to its mature fabrication process. If VCSELs can extend the available emission wavelengths into ultraviolet to visible regime, many more applications could benefit from such a light source. However, GaN-based short-wavelength VCSELs are still suffering from some challenges [3], [4].

Generally, AlGaAs-selective oxide layer employed in GaAs-based VCSELs not only achieves current confinement but also provides a stable refractive index variation in the lateral direction to improve light confinement [5]. GaAs-based VCSELs are very sensitive to this selective oxide structure. Changing the diameter, position, and the thickness of oxide layers may significantly influence the device performance. Therefore, the design and optimization of oxide-confined structure had been carried out extensively in experiment and theory [6], [7], [8], [9]. In comparison, selective oxidation is very difficult in GaN-based VCSELs due to the character of the material itself. In order to realize lateral current confinement in current injection GaN-based VCSELs, in general, a patterned insulating layer is deposited directly on the surface of p-GaN. However, this method will result in a convex shape structure, which will cause lateral diffraction and radiation loss, and we called it antiguiding effect [4], [10], [11]. In recent years, many research groups have developed various approaches to achieve better lateral confinement structure in GaN-based VCSELs by using ion implantation [12], [13], photoelectrochemically etched air-gap aperture [14], buried insulating layer [15], [16], [17], monolithic curved mirror [18], and reactive ion etching (RIE) passivation [19], [20]. Among them, insulator-buried structure is rather simple and preferable. The insulator-buried structure could not only provide good electrical confinement but also improve the optical confinement in the transverse direction. In 2018, Kuramoto et al. [15]. introduced a SiO_2-buried structure in GaN-based VCSEL with hybrid epitaxial/dielectric distributed Bragg reflector (DBR). The reported devices showed a high output power of 6 mW. The next year, they applied the same structure in 256-element blue VCSEL array and achieved a high output power of 1.19 W [21]. In our previous work, we also experimentally found that SiO_2-buried structure can effectively reduce the intracavity loss and improve the performance of GaN-based VCSELs [17]. However, this structure still lacks detailed study, and further investigation is required for its future practical use.

Manuscript received 30 June 2023; revised 10 August 2023; accepted 24 August 2023. Date of publication 8 September 2023; date of current version 24 October 2023. This work was supported in part by the National Natural Science Foundation of China under Grant U21A20493 and Grant 62234011, and in part by the National Key Research and Development Program of China under Grant 2017YFE0131500. The review of this article was arranged by Editor Y. Zhao. *(Corresponding author: Baoping Zhang.)*

Rongbin Xu and Baoping Zhang are with the Department of Microelectronics and Integrated Circuits, Optoelectronics Laboratory of Micro/nano-Optoelectronics, Xiamen University, Xiamen 361005, China (e-mail: bzhang@xmu.edu.cn).

Hidefumi Akiyama is with the Institute for Solid State Physics, The University of Tokyo, Kashiwa, Chiba 277-8581, Japan.

Color versions of one or more figures in this article are available at https://doi.org/10.1109/TED.2023.3309617.

Digital Object Identifier 10.1109/TED.2023.3309617

0018-9383 © 2023 IEEE. Personal use is permitted, but republication/redistribution requires IEEE permission.
See https://www.ieee.org/publications/rights/index.html for more information.

Authorized licensed use limited to: Xiamen University. Downloaded on October 27,2023 at 02:46:11 UTC from IEEE Xplore. Restrictions apply.

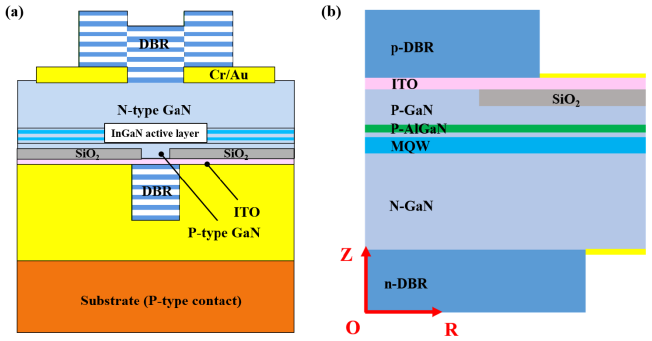

Fig. 1. (a) Schematic cross section of the GaN-based VCSEL with SiO_2-buried structure. (b) Simulation structure of resonant cavity, O, Z, and R, represent the original point, the vertical, and lateral coordinate of simulation model, respectively.

TABLE I
DETAIL LAYER STRUCTURE OF THE CALCULATED VCSEL

Material	Thickness (nm)	Doping concentration (cm^{-3})
Ta_2O_5/SiO_2	10× 50.93/78.77	--
n-GaN	1994.5	$2.5x10^{18}$
$In_{0.02}Ga_{0.98}N$	85	--
$In_{0.18}Ga_{0.82}N/GaN$	2× 2.5/6	--
$In_{0.03}Ga_{0.97}N$	85	--
p-$Al_{0.18}Ga_{0.82}N$	20	$1x10^{18}$
p-GaN	596	$4x10^{17}$
SiO_2	20	--
ITO	40	--
SiO_2/Ta_2O_5	12× 78.77/50.93	--

In this article, we have theoretically investigated both optical and electrical properties of GaN-based VCSEL with SiO_2-buried structure. The simulation results showed that the threshold current and slope efficiency of GaN-based VCSEL are remarkable impacted by modifying the SiO_2 thickness. However, the variation tendencies are different. When the SiO_2 layer becomes thicker, a better lateral optical confinement can be achieved, while the current confinement becomes worse. In addition, since the current injection area is also determined by SiO_2 layer, the devices with different aperture sizes were also investigated. This study provides reference significance for the realization of high-performance GaN-based VCSEL.

II. DEVICE STRUCTURE AND PHYSICAL MODEL

The geometry of the VCSEL is schematically illustrated in Fig. 1 and the detailed layer structure is summarized in Table I. The active region consists of two $In_{0.18}Ga_{0.82}N/GaN$ quantum wells (QWs) having a well and barrier thickness of 2.5 and 6 nm, respectively. A 20 nm $Al_{0.2}Ga_{0.8}N$ layer was used as electron blocking layer. The VCSEL has a dual dielectric DBR design, combining the ITO current spreading layer and SiO_2 insulating layer together. The studied VCSEL has the cavity length of $\sim 16\ \lambda$ and the current aperture with a diameter of 15 μm is defined by SiO_2.

To investigate the electrical and optical characteristics of SiO_2-buried structure VCSEL, an advanced simulator Crosslight PICS3D was utilized in this study. The PICS3D is based on 3-D finite element analysis and can be employed

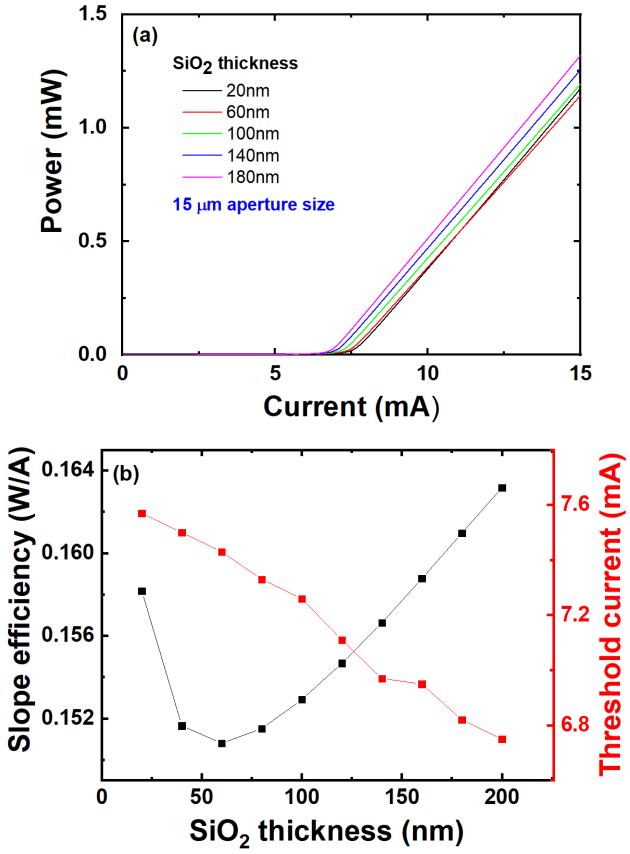

Fig. 2. (a) Simulated lasing power as a function of the injection current for devices with different SiO_2 thickness. (b) Slope efficiency and threshold as a function of the buried SiO_2 thickness at the current of 15 mA.

to solve the Poisson's equation, current continuity equations, carrier transport equations, complex wave equations, and rate equations of VCSEL devices in the cylindrical coordinates. The transport model includes drift and diffusion of electrons and holes, Fermi statistics, as well as spontaneous and defect-related Shockley—Read–Hall (SRH) recombination of carriers. The spontaneous and piezoelectric polarization in GaN-based materials were considered in the simulator to calculate the built-in polarization field. The polarization charge density is calculated to be around -1.2×10^{13} cm^{-2} [23], and the polarization level was set to 20% since the reduction of the interface charge may be screened by defects and other effects during the actual epitaxial growth and device fabrication. In the optical mode model, both the longitudinal and transverse optical modes are solved by the effective index model (EIM). The use of EIM model is beneficial to the device with complex structural variation in lateral direction. Since the cylindrical symmetry of the calculated VCSEL, the simulation model can be simplified into a 2-D axisymmetric structure, as shown in Fig. 1(b).

III. SIMULATION RESULTS AND DISCUSSION

The P–I curves of 15 μm aperture size VCSELs with different SiO_2 thickness are shown in Fig. 2(a). The fitting slope efficiency and threshold current are shown in Fig. 2(b). We can observe that the threshold current slightly decrease with the

Authorized licensed use limited to: Xiamen University. Downloaded on October 27,2023 at 02:46:11 UTC from IEEE Xplore. Restrictions apply.

increase of SiO_2 thickness. In addition, it is interesting that the fitting slope efficiency first decreases and then increases when increasing SiO_2 thickness. The simulation results show that GaN VCSELs with SiO_2-buried structure are sensitive to the thickness of SiO_2 layer, which is the same as oxide-confined GaAs VCSELs. The trends of threshold and slope efficiency can be attributed to the influence of different SiO_2 thickness on the lateral optical and current confinement capacity of devices, which will be discussed in the latter part of the article.

A. Lateral Optical Confinement

In VCSEL structure, the threshold condition and slope efficiency are strongly dependent on the lateral optical losses. Usually, the lateral optical confinement capacity of VCSEL can be estimated by using EIM [22]. The relative refractive index difference $\Delta n/n$ can be estimated from the local resonance wavelength shift between the center and peripheral region of the VCSEL mesa, as described by the following equation:

$$\frac{\lambda_c - \lambda_p}{\lambda_c} = \frac{\Delta\lambda}{\lambda_c} = \frac{\Delta n}{n} \tag{1}$$

where λ_c and λ_p are the resonance wavelengths of the center and peripheral areas, respectively. λ_c and λ_p can be obtained from the calculated reflectivity spectrum of an entire VCSEL cavity by transfer matrix simulation. Fig. 3(a) shows the calculated $\Delta n/n$ values for SiO_2-buried structure VCSELs at the central resonance wavelength of 445 nm as a function of SiO_2 thickness. It was found that the $\Delta n/n$ gradually increase with the increase of SiO_2 thickness. Fig. 3(b) shows the fundamental (LP_{01}) and first order (LP_{11}) optical modes within the QW of the devices with different SiO_2 thickness. The full width at half maximum (FWHM) of LP_{01} and LP_{11} mode distributions in the lateral direction were narrowed with the increase of SiO_2 thickness. This is because the increased $\Delta n/n$ leads to a better confinement to the optical modes. The theoretical Q value of lasers can be calculated by using the method reported in [24]. And the calculated Q value of VCSEL is increase from 1000 to 2356 with the increase of SiO_2 thickness. All these suggest that a better optical confinement scheme can be achieved when the SiO_2 layer becomes thicker, and finally achieved a lower threshold current and higher slope efficiency. However, it is important to note that a thicker SiO_2 layer may not always be better for VCSEL performance. With the increase of $\Delta n/n$, the strong guiding structure ($\Delta n > 0.03$) can cause an increase of diffraction loss [10], [11]. Thus, a moderate SiO_2 thickness ($\Delta n \approx 0.03$) is usually preferred in actual device design.

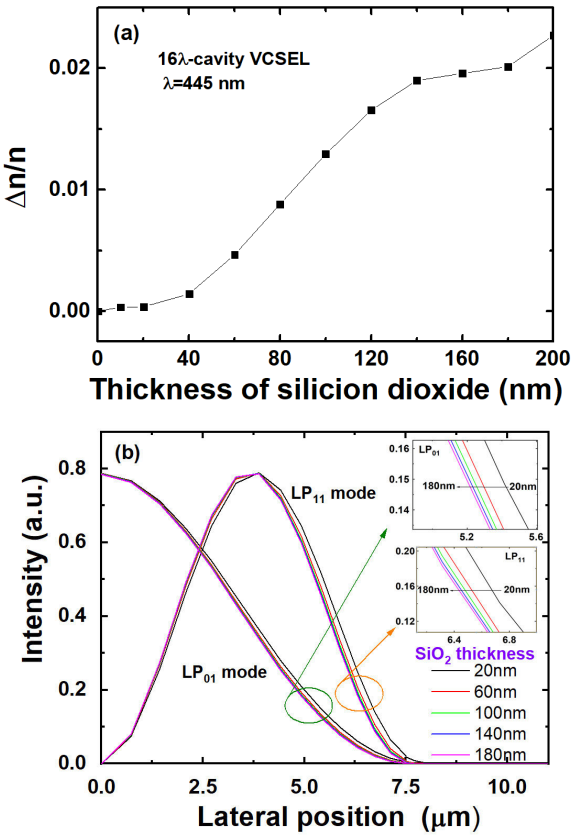

Fig. 3. (a) Relative refractive index difference as a function of SiO_2 thickness. (b) Optical mode distributions of LP_{01} and LP_{11} within the QW along the lateral direction. Insets show the zoom-in mode distributions curves of LP_{01} and LP_{11}.

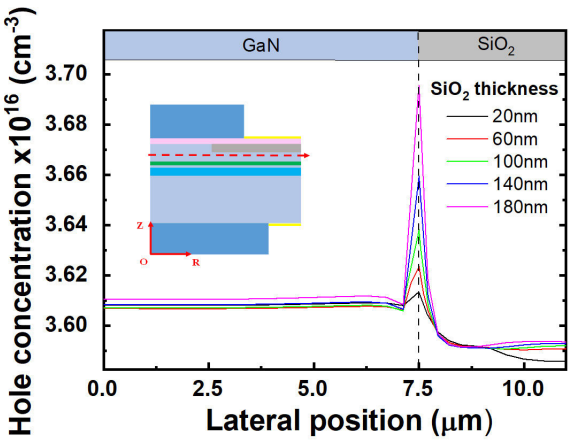

Fig. 4. Lateral hole concentrations in p-GaN below the SiO_2 layer at the current of 15 mA. The position is marked by red dashed line in the inset schematic VCSEL.

B. Lateral Current Confinement

In order to investigate the underlying mechanism of varying slope efficiency, we further discuss the lateral current confinement capacity of VCSEL with different SiO_2 thickness. Fig. 4 shows the lateral distributions of hole concentrations in p-GaN below the SiO_2 layer. As shown in Fig. 4, the accumulation of holes will be formed at the p-GaN/SiO_2 interface near the edge of current aperture. This accumulation effect becomes more obvious when the SiO_2 layer becomes thicker. The SiO_2/GaN structure in VCSEL will form a MOS-like heterostructure [25], and the difference in the polarization across the heterointerface will result in interface charge. It has been reported that the electrical properties of the MOS SiO_2/GaN structures could be affected by the existence of polarization charge on SiO_2/GaN interface [25], [26]. Thus, the accumulation of holes could be

Authorized licensed use limited to: Xiamen University. Downloaded on October 27,2023 at 02:46:11 UTC from IEEE Xplore. Restrictions apply.

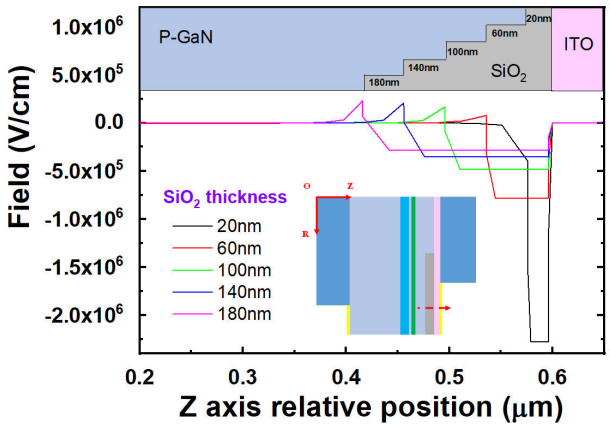

Fig. 5. Vertical electric field profiles for the VCSELs with different SiO_2 thickness. The position is marked by red dashed line in the inset schematic VCSEL.

attributed to the existence of polarization-induced electric field at the p-GaN/SiO_2 interface.

Fig. 5 shows vertical electric field profiles for the VCSELs with different SiO_2 thickness. The electric fields at the p-GaN/SiO_2 interface originate from applied bias and material polarization. The electric fields induced by applied bias and polarization are in opposite direction. When the SiO_2 thickness is thin (20 nm), the potential difference between SiO_2 layer is small, and thus the electric field originated from bias voltage can compensate the polarization electric field at the p-GaN/SiO_2 interface. However, when the SiO_2 layer becomes thicker, the potential difference becomes larger, the shielding of the polarization electric field at the p-GaN/SiO_2 interface is weaken. The unshielded polarization electric field at the p-GaN/SiO_2 interface will lead to the accumulation of holes below the SiO_2 layer, and thus led to the generation of leakage current. This leakage current is comprised of holes moving horizontally outward away from the center axis of the VCSEL, in the p-GaN layer, as shown in Fig. 6. This is the reason why the slope efficiency of VCSEL showed decrease when the thickness of SiO_2 layer is increased from 20 to 60 nm shown in Fig. 2(b). With even thicker SiO_2, the slop efficiency is improved. This is because the slope efficiency of VCSEL is affected by the injection efficiency and intracavity loss. Since the existence of leakage current, the injection efficiency first decreases with the increase of SiO_2 thickness, and thus the slope efficiency decreases. However, the thick SiO_2 layer can enhance lateral optical confinement, and the lateral optical loss can be reduced. Therefore, the slope efficiency of the simulated device showed first decrease and then increase, as shown in Fig. 2(b).

C. Effect of SiO_2 Aperture Size

In addition to the thickness of SiO_2, the current injection region is also determined by the patterned SiO_2 layer. In this part, the influence of current aperture size on the performance of SiO_2-buried structure VCSEL is considered.

Fig. 7 shows the spatial distributions of the current density (red lines), LP_{01} and LP_{11} mode distributions of the devices with 10 and 15 μm aperture diameters. As shown in Fig. 7, the

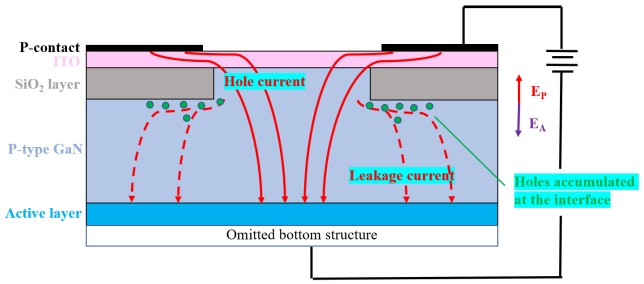

Fig. 6. Cartoon diagram illustrating hole leakage current outside the edge of current injection aperture in VCSEL. E_P and E_A are polarization and applied bias-induced electric field, respectively.

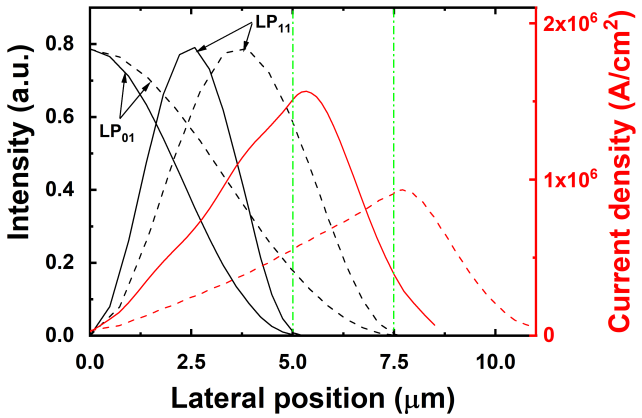

Fig. 7. Current density (red line) and optical mode (black line) distributions within the QWs along the lateral direction. The solid and dashed lines represent the VCSELs with 10 and 15 μm aperture diameters, respectively.

buried SiO_2 layer will cause current crowding, and the current density is maximized near the edge of the current injection aperture. Outside the current injection aperture, the current in QWs is comprised of the polarization-induced current and horizontal current diffusion. Since the high-order modes are distributed in the peripheral region of aperture, the nonuniform distribution of current density within the QW may favor higher order modes in such a confinement structure. However, due to the long-cavity structure and mode competition, higher order modes are suppressed and almost have no impact on the total slope efficiency, only LP_{01} and LP_{11} modes were considered during the simulation.

Fig. 8 shows the calculated P–I curves of LP_{01} and LP_{11} optical modes for the VCSELs with 10 and 15 μm aperture diameters. Two transverse modes can lase simultaneously for both devices. The increasing rate of LP_{11} mode is higher than that of LP_{01} mode due to the nonuniform current distribution, as shown in Fig. 7. It is obviously that the devices with 10 μm aperture size have small threshold current due to the higher injection current density.

We further compare the slope efficiency of lasing modes for the devices with 10 and 15 μm aperture sizes, as shown in Fig. 9. The slope efficiency variation tendencies of LP_{01} and LP_{11} modes are the same as that in Fig. 2(b). The device with small (10 μm) aperture size has a low slope efficiency. In addition, contrast to the device with 20 nm SiO_2 layer, the slope efficiency of LP_{01} and LP_{11} modes for 15 μm aperture

Authorized licensed use limited to: Xiamen University. Downloaded on October 27,2023 at 02:46:11 UTC from IEEE Xplore. Restrictions apply.

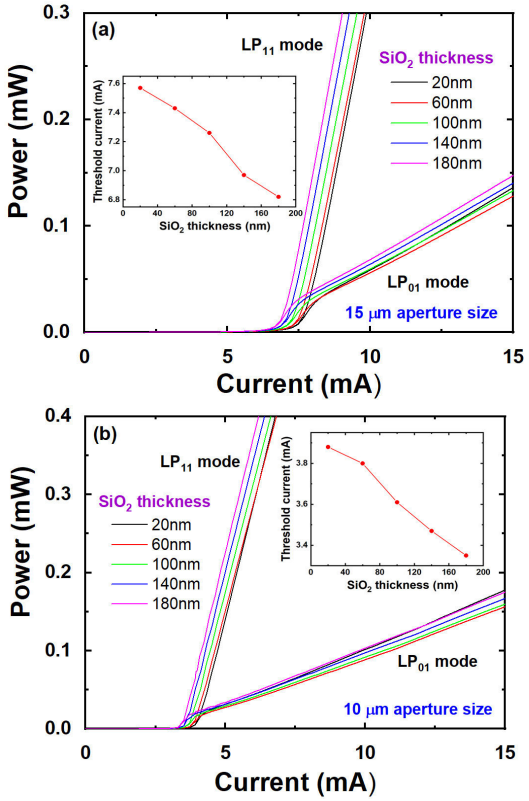

Fig. 8. *P–I* curves of LP_{01} and LP_{11} lasing modes for the devices with different SiO_2 thickness. (a) 15 μm aperture size. (b) 10 μm aperture size. Insets show the threshold current in terms of the SiO_2 thickness.

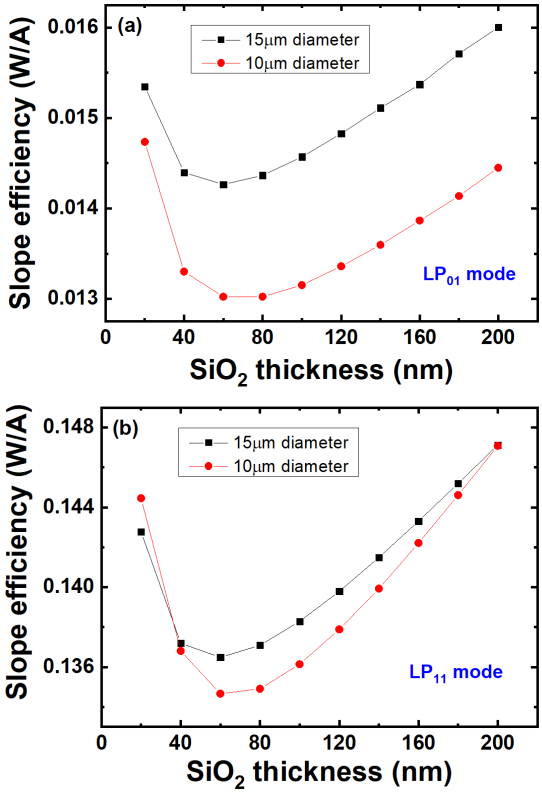

Fig. 9. Slope efficiency of (a) LP_{01} mode and (b) LP_{11} mode as a function of SiO_2 thickness of the devices with 10 and 15 μm aperture sizes.

size device with 60 nm SiO_2 are decreased by 7.1% and 4.4%, respectively, while the 10 μm aperture size devices are decreased by 11.6% and 6.8%. Since injection current is concentrated distribution at the edge of the aperture, the LP_{01} mode is more susceptible to the leakage current. Therefore, because of the higher injection current density, the leakage current has a bigger influence on the SiO_2-buried structure VCSEL with small aperture size, especially for the LP_{01} lasing mode.

IV. Conclusion

In conclusion, this work provides a deeper understanding on the influence of SiO_2 layer in GaN-based VCSELs with SiO_2-buried structure. The threshold condition and the slope efficiency of VCSEL is strongly dependent on the lateral optical and current confinement caused by the SiO_2 layer. We have found that a better optical confinement scheme can be achieved when the SiO_2 layer becomes thicker. However, due to the special polarization property of GaN material, thick SiO_2 layer will lead to the accumulation of holes at the p-GaN/SiO_2 interface, resulting in leakage current. As a consequence, the slope efficiency of device exhibits an abnormal trend of decreasing initially and then increasing when the SiO_2 becomes thicker. Moreover, the variation of slope efficiency is more significant since the current density is larger for VCSELs with small aperture size. Therefore, it is important that a proper design of SiO_2 layer in VCSEL with SiO_2-buried structure is needed to avoid the effect of leakage current, especially for device with small aperture size. This work provides important significance for the development of high-performance GaN-based VCSELs.

References

[1] J. S. Harris, T. O'sullivan, T. Sarmiento, M. M. Lee, and S. Vo, "Emerging applications for vertical cavity surface emitting lasers," *Semiconductor Sci. Technol.*, vol. 26, no. 1, Jan. 2011, Art. no. 014010, doi: 10.1088/0268-1242/26/1/014010.

[2] Å. Haglund et al., "Progress and challenges in electrically pumped GaN-based VCSELs," *Proc. SPIE*, vol. 9892, pp. 161–180, Apr. 2016, doi: 10.1117/12.2229428.

[3] H.-C. Yu et al., "Progress and prospects of GaN-based VCSEL from near UV to green emission," *Prog. Quantum Electron.*, vol. 57, pp. 1–19, Jan. 2018, doi: 10.1016/j.pquantelec.2018.02.001.

[4] C.-Y. Huang, K.-B. Hong, Z.-T. Huang, W.-H. Hsieh, W.-H. Huang, and T.-C. Lu, "Challenges and advancement of blue III-nitride vertical-cavity surface-emitting lasers," *Micromachines*, vol. 12, no. 6, p. 676, Jun. 2021, doi: 10.3390/mi12060676.

[5] B. Weigl et al., "High-performance oxide-confined GaAs VCSELs," *IEEE J. Sel. Topics Quantum Electron.*, vol. 3, no. 2, pp. 409–415, Apr. 1997, doi: 10.1109/2944.605686.

[6] R. P. Sarzała, "Optimization of oxide-confined vertical-cavity surface-emitting diode lasers," *Semiconductor Sci. Technol.*, vol. 22, no. 2, pp. 113–118, Feb. 2007, doi: 10.1088/0268-1242/22/2/019.

[7] M. Alias, S. Shaari, and S. Mitani, "Optimization of electro-optical characteristics of GaAs-based oxide confinement VCSEL," *Laser Phys.*, vol. 20, pp. 806–810, Mar. 2010, doi: 10.1134/S1054660X10070017.

[8] M. Yazdanypoor and A. Gholami, "Optimizing optical output power of single-mode VCSELs using multiple oxide layers," *IEEE J. Sel. Topics Quantum Electron.*, vol. 19, no. 4, pp. 1701708–170176s8, Jul. 2013, doi: 10.1109/JSTQE.2013.2252002.

[9] F. A. I. Chaqmaqchee, and J. A. Lott, "Impact of oxide aperture diameter on optical output power, spectral emission, and bandwidth for 980 nm VCSELs," *OSA Continuum*, vol. 3, no. 9, pp. 2602–2613, Sep. 2020, doi: 10.1364/OSAC.397687.

Authorized licensed use limited to: Xiamen University. Downloaded on October 27,2023 at 02:46:11 UTC from IEEE Xplore. Restrictions apply.

[10] E. Hashemi et al., "Engineering the lateral optical guiding in gallium nitride-based vertical-cavity surface-emitting laser cavities to reach the lowest threshold gain," *Jpn. J. Appl. Phys.*, vol. 52, no. 8S, May 2013, Art. no. 08JG04, doi: 10.7567/JJAP.52.08JG04.

[11] E. Hashemi et al., "Analysis of structurally sensitive loss in GaN-based VCSEL cavities and its effect on modal discrimination," *Opt. Exp.*, vol. 22, no. 1, pp. 411–426, Jan. 2014, doi: 10.1364/OE.22.000411.

[12] J. T. Leonard et al., "Nonpolar III-nitride vertical-cavity surface-emitting lasers incorporating an ion implanted aperture," *Appl. Phys. Lett.*, vol. 107, no. 1, Jul. 2015, Art. no. 011102, doi: 10.1063/1.4926365.

[13] S. M. Mishkat-Ul-Masabih, A. A. Aragon, M. Monavarian, T. S. Luk, and D. F. Feezell, "Electrically injected nonpolar GaN-based VCSELs with lattice-matched nanoporous distributed Bragg reflector mirrors," *Appl. Phys. Exp.*, vol. 12, no. 3, Feb. 2019, Art. no. 036504, doi: 10.7567/1882-0786/ab0576.

[14] J. T. Leonard et al., "Nonpolar III-nitride vertical-cavity surface-emitting laser with a photoelectrochemically etched air-gap aperture," *Appl. Phys. Lett.*, vol. 108, no. 3, Jan. 2016, Art. no. 031111, doi: 10.1063/1.4940380.

[15] M. Kuramoto et al., "Enhancement of slope efficiency and output power in GaN-based vertical-cavity surface-emitting lasers with a SiO_2-buried lateral index guide," *Appl. Phys. Lett.*, vol. 112, no. 11, Mar. 2018, Art. no. 111104, doi: 10.1063/1.5020229.

[16] R. Iida et al., "GaN-based vertical cavity surface emitting lasers with lateral optical confinements and conducting distributed Bragg reflectors," *Jpn. J. Appl. Phys.*, vol. 59, no. SG, Feb. 2020, Art. no. SGGE08, doi: 10.35848/1347-4065/ab6e05.

[17] R. Xu et al., "Effects of lateral optical confinement in GaN VCSELs with double dielectric DBRs," *IEEE Photon. J.*, vol. 12, no. 2, pp. 1–8, Apr. 2020, doi: 10.1109/JPHOT.2020.2979564.

[18] T. Hamaguchi et al., "Lateral optical confinement of GaN-based VCSEL using an atomically smooth monolithic curved mirror," *Sci. Rep.*, vol. 8, no. 1, pp. 1–8, Jul. 2018, doi: 10.1038/s41598-018-28418-6.

[19] M. Kuramoto, S. Kobayashi, T. Akagi, K. Tazawa, H. Tanaka, and T. Takeuchi, "Nano-height cylindrical waveguide in GaN-based vertical-cavity surface-emitting lasers," *Appl. Phys. Exp.*, vol. 13, no. 8, Jul. 2020, Art. no. 082005, doi: 10.35848/1882-0786/aba45b.

[20] G. Cosendey, A. Castiglia, G. Rossbach, J.-F. Carlin, and N. Grandjean, "Blue monolithic AlInN-based vertical cavity surface emitting laser diode on free-standing GaN substrate," *Appl. Phys. Lett.*, vol. 101, no. 15, Oct. 2012, Art. no. 151113, doi: 10.1063/1.4757873.

[21] M. Kuramoto et al., "Watt-class blue vertical-cavity surface-emitting laser arrays," *Appl. Phys. Exp.*, vol. 12, no. 9, Aug. 2019, Art. no. 091004, doi: 10.7567/1882-0786/ab3aa6.

[22] G. R. Hadley, "Effective index model for vertical-cavity surface-emitting lasers," *Opt. Lett.*, vol. 20, no. 13, pp. 1483–1485, Jul. 1995, doi: 10.1364/OL.20.001483.

[23] J.-R. Chen et al., "Numerical study of optical properties of InGaN multi-quantum-well laser diodes with polarization-matched AlInGaN barrier layers," *Appl. Phys. B, Lasers Opt.*, vol. 95, no. 1, pp. 145–153, Apr. 2009, doi: 10.1007/s00340-008-3331-9.

[24] J. S. Gustavsson, J. A. Vukusic, J. Bengtsson, and A. Larsson, "A comprehensive model for the modal dynamics of vertical-cavity surface-emitting lasers," *IEEE J. Quantum Electron.*, vol. 38, no. 2, pp. 203–212, Feb. 2002, doi: 10.1109/3.980274.

[25] P. Chen, S. J. Chua, W. D. Wang, D. Z. Chi, Z. L. Miao, and Y. D. Zheng, "Influence of the polarization on interfacial properties in $Al/SiO_2/GaN/Al_{0.4}Ga_{0.6}N/GaN$ heterojunction metal–insulator–semiconductor structures," *J. Appl. Phys.*, vol. 94, no. 7, pp. 4702–4704, Oct. 2003, doi: 10.1063/1.1599046.

[26] J. Zhang, C. Hitchcock, Z. Li, and T. P. Chow, "Investigation of pyroelectric polarization effect on GaN MOS capacitors and field-effect transistors," in *Proc. Lester Eastman Conf. High Perform. Devices (LEC)*, Aug. 2012, pp. 1–4, doi: 10.1109/lec.2012.6410982.

Authorized licensed use limited to: Xiamen University. Downloaded on October 27,2023 at 02:46:11 UTC from IEEE Xplore. Restrictions apply.